8 Parathyroid Gland

Abdelhamid H. Elgazzar

8.1 Introduction

The last organ to be recognized in man, the parathyroid glands, was discovered in 1880 by Ivar Sandstrom, a Swedish medical student. The discovery attracted little attention initially. Later, with the uncovering of the relationship of the glands to significant bone disease, interest quickened. In the early 1900s, Jacob Erdheim demonstrated that the four parathyroid glands were enlarged in osteomalacia and in rickets and thought it was a compensatory phenomenon. Subsequently, occasional cases of bone disease were encountered in which only a single gland was enlarged. In 1915, Friedrich Schlaugenhaufer suggested that enlargement of a single parathyroid gland might be the cause of the bone disease, not its result. The first parathyroidectomy for von Recklinghausen's disease of bone was performed by Felix Mandl in 1925 in Vienna. Subsequently, the parathyroid glands were shown to be affected by a number of primary pathological processes – neoplasia (adenoma and carcinoma) and hyperplasia (wasserhelle-cell and chief-cell types) – that resulted in overactivity and required surgical removal of one or more of them [1].

The frequency of hyperparathyroidism has been increasing in the past few decades. It has also been recognized that this condition has various clinical presentations and can be associated with normocalcemia or borderline hypercalcemia. The condition, even with atypical laboratory findings, is known to be associated with an increasing number of complications, including the more recent findings of the resultant neuromuscular and psychiatric disorders. Accordingly, the management of hyperparathyroidism by the proper surgical approach is crucial. Although the success rate of surgical excision of abnormal parathyroid glands is high, certain factors and new developments favor preoperative identification of abnormal glands [2–7]. Exploring the pathophysiology of the parathyroids can help to enhance our understanding of the currently used preoperative localization procedures and their future modifications. Optimal parathyroid scintigraphy requires an understanding of (a) the embryologic, anatomic, and physiologic features of the parathyroid glands and (b) the properties of the two common imaging agents, ^{99m}technetium-sestamibi and ^{99m}Tc-tetrofosmin. Normal parathyroid glands are too small to be visualized, but parathyroid disease often produces visibly enlarged glands. Enlarged parathyroid glands may be found near the thyroid gland or outside their expected locations. Characteristic abnormal scintigraphic patterns may be described as focal or multifocal, usual or ectopic in location, and associated with a normal or abnormal thyroid gland. Patients who are referred for parathyroid imaging should have an abnormal biochemical profile. The first step in evaluating images of a patient suspected of having parathyroid disease is to correlate the normal or abnormal scintigraphic patterns with the clinical and surgical history. By integrating the interpretative, pathophysiologic and technical data of parathyroid scintigraphy, the interpreting physician can be more confident of establishing a correct diagnosis and

can precisely guide the surgeon to a single parathyroid adenoma, multiple parathyroid adenomas, or multigland hyperplasia [8].

8.2 Anatomical and Physiological Considerations

Normal parathyroid glands are derived from the pharyngeal pouches, the upper glands from the endoderm of the fourth pouch and the lower glands from the third pouch. The parathyroid glands are typically located on the thyroid gland (Fig. 8.1). Occasionally one or more glands may be embedded in the thyroid [9]. The normal position of the superior parathyroids is at the cricothyroid junction, above the anatomic demarcation of the inferior thyroid artery and the recurrent laryngeal nerve [10, 11]. The inferior parathyroids are more widely distributed, with most of them anterolateral or posterolateral to the lower thyroid gland [11]. The accessory glands that can be variously located in human beings, from the cricoid cartilage down into the mediastinum [12, 13], are derived from the numerous dorsal and ventral wings of the pouches. Normally, human beings have four glands, but more or fewer than this number are found in some individuals [2]. Among healthy adults, 80% – 97% have four parathyroids, approximately 5% have fewer than four glands, and 3% – 13% have supernumerary glands [11].

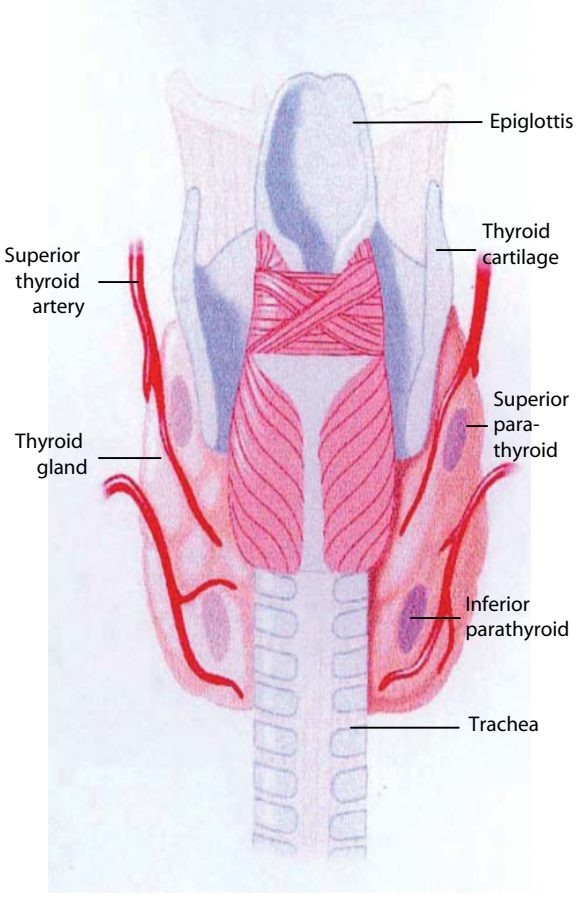

Fig. 8.1. Diagram showing typical locations of parathyroid glands

The normal glands vary considerably in shape and size between individuals and within the same individual. Because of the variable shapes of the parathyroids, the diameters vary. The normal glands usually measure 4 – 6 mm in length, 2 – 4 mm in width, and 0.5 – 2 mm in thickness. The glands are usually ovoid or bean-shaped but may be elongated, flattened into a leaf-like structure, or multi-lobulated [3]. The weight of the glands is therefore a better estimate of the glandular tissue; they are usually 30 mg each, with the largest normal gland not exceeding 70 mg. The relatively new important parameter, the weight of the functioning parenchyma, can be calculated from the glandular weight and the relative proportions of the two main glandular components, parenchymal and fat cells. The total weight of the glands is less than 210 mg and the total parenchymal cell weight is less than 145 mg [3]. The proportion of fat cells in the parathyroid glands varies with age, since they are sparse up to adolescence and increase gradually to constitute 10% – 25% of the glandular volume by the age of 30: the proportion remains fairly constant except when the individual suffers from obesity, which causes a larger amount of fat cells, as opposed to cachectic persons who have essentially no fat cells. In normal glands, parenchymal cells are predominantly chief cells which contain cytoplasmic fat droplets. Oxyphilic and transitional oxyphilic cells are sparsely present in children and young adults and increase to 4% – 5% of the parenchymal cells in old age. These cells tend to form nodules if they increase in number and have a very small amount of fat or no fat at all in their cytoplasm. Ultrastructurally, oxyphil cells are characterized by the presence of closely packed mitochondria while chief cells contain moderate to high mitochondrial content, but also prominent Golgi body and endoplasmic reticulum. Water-clear cells are vacuolated with distended organelles. Each of the three cell types may contain varying amounts of lipid droplets and residual bodies.

Table 8.1 summarizes the types of parathyoid cells and their function.

Parathyroid hormone has four principal actions: (a) to increase calcium absorption from the gastrointestinal tract; (b) to stimulate osteoclastic activity, resulting in resorption of calcium and phosphate from bone; (c) to inhibit phosphate reabsorption by the proximal renal tubules; and (d) to enhance renal tubular calcium reabsorption. Parathyroid hormone secretion is controlled mainly by the extracellular calcium concentra-

Table 8.1. Cells of the parathyroid glands and their functions

Cell type	Major ultrastructural feature	Function
Chief cell	Slightly eosinophilic cytoplasm, few mitochondria	The active endocrine cell, producing the parathyroid hormone
Oxyphil cell	Rich eosinophilic cytoplasm, tightly packed mitochondria	May be able to produce parathyroid hormone
Transitional oxyphil cell	Less eosinophilic cytoplasm	Variant of oxyphil cell
Clear cell	Foamy and water-clear cytoplasm	Unknown, fundamentally inactive

tion. The parathyroid cell surface is thought to be equipped with a cation-sensitive receptor mechanism through which ambient calcium regulates the cytosolic calcium ($Ca^{2+}i$) concentration and parathyroid hormone secretion. Activation of this receptor also causes activation of protein kinase C [3]. 1,25-Dihydroxycholecalciferol reduces the secretion of parathyroid hormone independent of any changes in calcium concentration. Parathyroid hormone is metabolized in Kupffer's cells of the liver.

In patients with hyperparathyroidism, pathological parathyroid cells show defective sensing of ambient calcium. The cellular basis of this abnormality is unknown, although increased protein kinase C activity within abnormal parathyroid cells may be the mechanism. Pathological parathyroid glands also have an increased parenchymal cell content, although the extent of hypercalcemia appears more closely related to the defective secretory regulation than to increased parenchymal cell mass [5, 14].

8.3 Hyperparathyroidism

Hyperparathyroidism has been diagnosed with increasing frequency in recent years due to awareness of the disease and to the laboratory advancement that allowed for routine chemistry screening. The condition is characterized by excess secretion of parathyroid hormone. The resulting biochemical changes, including increased levels of serum calcium and increased urinary excretion of calcium, may result in calcium wastage, nephrocalcinosis, urolithiasis, bone disease, and neuropsychiatric disturbances. Hyperparathyroidism may occur as a primary, secondary, or tertiary disease. It can also occur as eutopic and ectopic disease. In addition, it may have a familial origin, as in multiple endocrine neoplasia (MEN).

8.3.1 Primary Hyperparathyroidism

Primary hyperparathyroidism occurs due to neoplastic or hyperplastic parathyroid glands or when nonparathyroid tumors such as bronchogenic or renal cell carcinomas secrete ectopically parathyroid hormone or a biologically similar product. The incidence in the USA has been estimated at approximately 27.7 cases per 100,000 population per year [15]. The condition is more prevalent in females than males by a ratio of 3 to 1. More than 80% of patients with primary hyperparathyroidism have a solitary adenoma. Hyperplasia – predominantly of chief cells – occurs in less than 20% of patients. Parathyroid carcinoma is the cause in less than 1% of patients, and very rarely the condition is due to ectopic secretion of parathyroid hormone such as with renal cell carcinomas.

Primary hyperparathyroidism occurs as part of MEN. MEN is a hereditary syndrome that involves hyperfunctioning of two or more endocrine organs. Primary hyperparathyroidism, pancreatic endocrine tumors, and anterior pituitary gland neoplasms characterize type 1 MEN. MEN 2A is defined by medullary thyroid carcinoma, pheochromocytoma (about 50%), and hyperparathyroidism caused by parathyroid gland hyperplasia (about 20%). MEN 2B is defined by medullary thyroid tumor and pheochromocytoma. Both MEN 1 and MEN 2 are inherited autosomal dominant cancer syndromes. The gene responsible for MEN 1 is a tumor suppressor gene located on chromosome 11.

Primary hyperparathyroidism is the most common manifestation of MEN-1 (80% occurrence) and is caused by hyperplasia of all four parathyroid glands. This is followed by pancreatic islet cell tumors and involvement of the pituitary gland [16–19]. There is a high frequency of carcinoid tumors of foregut origin with male predominance for thymic involvement and female predominance for bronchial lesions [17, 20]. Type 1 MEN has a potentially lethal outcome with hemorrhagic peptic ulcer disease and metastatic pancreatic neoplasms [17]. Primary hyperparathyroidism is also associated with thyroid pathology in 15%–70% of patients [21–28]. This includes thyroid carcinoma, which has been reported in the range of 1.7%–6.2% (Table 8.2) of patients with primary hyperparathyroidism [21–31].

8.3.2 Secondary Hyperparathyroidism

Secondary hyperparathyroidism occurs when there is a condition causing chronic hypocalcemia such as chronic renal failure, malabsorption syndromes, dietary rickets, and ingestion of drugs such as phenytoin, phenobarbital, and laxatives, which decrease intestinal

Table 8.2. Incidence of thyroid cancer among patients with primary hyperparathyroidism: cumulative literature data

Author	Year	No. of patients	% with thyroid cancer
Ogburn [29]	1956	230	4 (1.7%)
Nishiyama [22]	1979	420	13 (3%)
Prinz [23]	1982	351	16 (4.6%)
Hedman [30]	1984	426	25 (5.8%)
Attie [24]	1992	948	31 (3.3%)
Burmeister [25]	1997	700	18 (2.6%)
Sidhu [26]	2000	65	4 (6.2%)
Bentrem [27]	2002	580	12 (2%)
Beus [31]	2004	101	3 (3%)
Total		3821	126 (3.3%)

absorption of calcium. Secondary hyperparathyroidism is simply a compensatory hyperplasia in response to hypocalcemia. In this condition, reduced renal production of 1,25-dihydroxyvitamin D_3 (active metabolite of vitamin D) leads to decreased intestinal absorption of calcium, resulting in hypocalcemia. Tubular failure to excrete phosphate results in hyperphosphatemia. Hypocalcemia along with hyperphosphatemia is compensated for by hyperplasia of the parathyroids to overproduce PTH [32].

8.3.3 Tertiary Hyperparathyroidism

Tertiary hyperparathyroidism describes the condition of patients who develop hypercalcemia following long-standing secondary hyperparathyroidism due to the development of autonomous parathyroid hyperplasia, which may not regress after correction of the underlying condition, as with renal transplantation.

8.3.4 Eutopic Parathyroid Disease

Parathyroid disease with typical location of glands (eutopic) represents 80% – 90% of all cases [33]. There is a relatively fixed location for the superior parathyroids and they are found close to the dorsal aspect of the upper thyroid [10, 11]. On the other hand, inferior parathyroids have a more widespread distribution, which is closely related to the migration of the thymus. Inferior parathyroids are mostly located inferior, posterior, or lateral to the lower thyroid [10]. They may be very close to the thyroid and may be covered by or attached to the thyroid capsule and are sometimes adjacent to or surrounded by remnant thymic tissue. Interestingly, the parathyroid glands demonstrate a remarkably constant symmetry, which is helpful in the surgical exploration of eutopic disease [11].

8.3.5 Ectopic Parathyroid Disease

Superior parathyroid adenoma may have an abnormal superoposterior mediastinal position, such as a retropharyngeal, retroesophageal, or paraesophageal site or the tracheo-esophageal groove. The frequency of ectopia (up to 39%) is similar for the right and left superior parathyroids [33]. Intrathyroid superior parathyroid adenomas are rare.

The more common ectopic inferior parathyroids are a well-established entity responsible for 10% – 13% of all cases of hyperparathyroidism [33]. Ectopic tissue can occur from the angle of the mandible to the mediastinum according to the developmental and migratory aberrations. These sites include the mediastinum, thymus, aortopulmonary window, carotid bifurcation and rarely thyroid, carotid sheath, vagus nerve, retroesophageal region, thyrothymic ligament, and pericardium [33 – 36].

8.3.6 Parathyroid Adenoma

Parathyroid adenoma is a benign tumor that is usually solitary, although multiple adenomas have been reported in a low percentage. The tumor varies in weight from less than 100 mg to more than 100 g. The most commonly found adenomas, however, weigh 300 mg–1 g. The size was found to correlate to the degree of hypercalcemia [5].

Microscopically, the vast majority of typical adenomas are formed predominantly of chief cells, although a mixture of oxyphil cells and transitional oxyphil cells is also common. Adenomas formed of water-clear cells are very rare. A rim of parathyroid tissue is usually present outside the capsule of the adenoma and can serve to distinguish it from parathyroid carcinoma. The chief cells in adenomas are usually enlarged, and their nuclei are larger and more variable in size than in normal chief cells. Nuclear pleomorphism may be prominent; this is not considered a sign of malignancy but a criterion for discriminating adenoma from hyperplasia, which lacks this feature. The following variants of parathyroid adenoma may be recognized:

8.3.6.1 Solitary Adenoma

Solitary adenoma is found in 80% – 85% of patients with primary hyperparathyroidism [11]. There is no significant predominance in location among the four parathyroids with each responsible for approximately 25% of all solitary adenomas [33]. The remainder of parathyroid glands associated with single adenomas usually have lower weight and parenchymal cell mass

than the average normal glands and show signs of secretory inactivity on electron microscopy [3].

8.3.6.2 Double or Multiple Adenomas

Double or multiple adenomas occur in up to 12% of cases of primary hyperparathyroidism [37, 38]. Double adenomas are bilateral in 55% – 88% of cases and are seen predominantly in patients beyond the 6th decade of life [39]. These patients have more prominent symptoms and usually have higher parathyroid hormone and alkaline phosphatase levels than those with a solitary parathyroid adenoma or hyperplasia. However, symptoms and laboratory values do not enable the diagnosis of double adenoma. Preoperative detection of double or multiple adenomas with any imaging modality is not reliable [40]. ^{99m}Tc-sestamibi scintigraphy has a sensitivity of less than 37% for detection of multisite disease [41, 42].

8.3.6.3 Cystic Adenoma

Cystic adenomas are thought to represent central necrosis or cystic degeneration of adenomas and account for less than 9% of all parathyroid adenomas [43]. Contrary to the asymptomatic true parathyroid cysts, which are due to embryologic vestiges of the third and fourth pharyngeal pouches or enlargement of microcysts within the parathyroid as a manifestation of colloid retention [43, 44], cystic adenomas are frequently associated with hyperparathyroidism. Cystic adenoma may not be visualized on sestamibi studies.

8.3.6.4 Lipoadenoma

Parathyroid lipoadenoma, composed of hyperfunctioning parathyroid tissue and fatty stroma [45], is a rare entity that occurs in patients beyond the 4th decade of life [45]. Compared to typical adenoma, there is no gender predilection and no difference in terms of symptoms. On ^{99m}Tc-sestamibi studies, the target-to-background signal ratio of lipadenoma may be low due to the high adipose content of the tumor [45].

8.3.6.5 Oncocytic Adenoma

In contrast to the typical adenoma that is composed of chief cells or a mixture of chief, oxyphil or transitional oxyphil cells, oncocytic adenoma is formed of exclusively oxyphil cells or of more than 80% of such cells. It is a rare subtype and has been reported to be associated with hyperparathyroidism. It is found in the sixth or seventh decades and like the typical adenomas is more common in women [46].

Table 8.3. Classification of parathyroid hyperplasia

Type	Major pathological features
Primary hyperplasia	Uniform chief cells with some oxyphil and transitional oxyphil cells
Secondary hyperplasia	
Diffuse (classic) type	Cords, sheets, or follicular arrangement of cells replacing the stromal fat cells. Oxyphil cells are more frequent in this type. This type is indistinguishable from the primary type
Adenomatous-nodular type	Cells are grouped in large islands or nodules. Necrosis is seen more frequently than in diffuse type

8.3.7 Parathyroid Hyperplasia

Parathyroid hyperplasia affects the glands to varying degrees, and commonly one or two glands are of normal size even though microscopic signs of endocrine hyperfunction, described later, are present, at least focally, in all glands. Chief cell hyperplasia is the most common and is composed of chief cells or a mixture of chief cells and to a lesser extent oxyphil cells. The cells are arranged diffusely, in nodules, or there is a mixture of both patterns. Water-clear cell hyperplasia is rare and is characterized by substantial enlargement of most parathyroid glands. The large water-clear cells are usually arranged in a diffuse pattern.

In primary hyperparathyroidism, hyperplasia affects the glands asymmetrically. In secondary hyperparathyroidism, the hyperplastic glands are more uniformly enlarged than with primary chief cell hyperplasia, with two histological types (Table 8.3). In the tertiary form, the glands are more often markedly and asymmetrically enlarged with frequent prominent parenchymal cell nodules.

Pathologically, it is difficult to differentiate primary chief cell hyperplasia of only one gland from adenoma. Both contain large numbers of active chief cells with cells characterized by aggregated arrays of rough endoplasmic reticulum and a large, complex Golgi apparatus with numerous vacuoles and vesicles. Secretory granules are frequently present in these cells. These changes indicate that most of these cells are in the more active phases of parathyroid hormone synthesis and secretion [47]. Molecular biology techniques used on pathological parathyroid tissue have shown that cell proliferation is monoclonal in many sporadic adenomas and in the largest glands of multiple endocrine neoplasia type I. This monoclonality has not been found in the smaller parathyroid glands of multiple endocrine neoplasia or in sporadic hyperplasia. Additionally, rearrangement of

parathyroid hormone gene in chromosome 11 was observed in sporadic adenomas [48].

8.3.8 Parathyroid Carcinoma

Parathyroid carcinoma is a rare cause of hyperparathyroidism which can arise in any parathyroid gland, including ectopic and mediastinal, although the usual site of involvement is the normally located parathyroids. The tumor is found predominantly in patients between the ages of 30 and 60 years, with no sex preference, and is usually functioning. The tumors tend to be larger than adenomas and appear as lobulated, firm, and uncapsulated masses that often adhere to the surrounding soft tissue structures [49]. The involved glands usually weigh more than 1 g and the diagnosis is restricted histologically to the lesions displaying infiltrative growth into vessel or capsule, since pleomorphism can be seen in many adenomas.

8.3.9 Hyperfunctioning Parathyroid Transplant

Autotransplantation of parathyroid tissue is performed in cases of recurrent, persistent type 1 MEN and symptomatic secondary hyperparathyroidism [19] in association with total parathyroidectomy. After total parathyroidectomy, the most normal glands, usually one or two, are used for the graft. They are diced into small fragments approximately 1–2× 1× 1 mm, with each fragment placed in an individual bed beneath the muscle sheath and between muscle fibers [19, 50]. The graft consists of a cluster of 10–25 parathyroid fragments. The remainder of the healthy gland (or glands) is cryopreserved for potential retransplantation [19, 40, 50]. Graft may be placed into the brachioradial muscle or flexor muscle group of the forearm or into the sternocleidomastoid muscle. A graft site in the forearm is preferred for accessibility for laboratory work-up of parathyroid hormone levels and surgical reexploration in cases of recurrent hyperparathyroidism [19]. The graft may be functional in 8–9 days after surgery [39].

After autotransplantation, recurrent hyperparathyroidism occurs in approximately 14% of cases [51]. The hyperfunctioning transplant is a possible cause as is residual or ectopic diseased parathyroid tissue. A hyperfunctioning graft in the forearm is easily demonstrated with Doppler US or ^{99m}Tc-sestamibi scintigraphy [19, 52].

8.4 Consequences of Hyperparathyroidism

Excess secretion of parathyroid hormone promotes bone resorption and consequently leads to hypercalcemia and hypophosphatemia. The clinical presentation and complications of hyperparathyroidism depends on the rapidity of development and the degree of hypercalcemia. The following abnormalities may occur:

- Genitourinary: nephrolithiasis, nephrocalcinosis, renal insufficiency, polyuria, nocturia and decreased urine concentrating ability.
- Gastrointestinal: Nausea, vomiting, constipation, increased thirst, loss of appetite, abdominal pain, peptic ulcers, heartburn (hypercalcemia causes increased gastric acidity) and pancreatitis.
- Musculoskeletal: myopathy, muscle weakness, osteoporosis, osteomalacia, bone and joint pains, renal osteodystrophy and pseudogout. In all forms of hyperparathyroidism there is increased bone resorption associated with increased osteoblastic activity, leading to increased uptake of bone-seeking radiopharmaceuticals. See also Chapter 6.
- Neuropsychiatric: Memory loss, anxiety, sleepiness, confusion, lassitude, coma, depression, impaired thinking and psychosis.
- Others: Fatigue, hypertension, pruritis, metastatic calcification including cardiocalcinosis and band keratopathy (present in the medial and lateral aspects of the cornea).

The five disease specific symptoms are muscle weakness, polydipsia, dry skin and itching, memory loss and anxiety. Overall the symptoms, particularly the disease specific ones, show significant decline after successful parathyroidectomy [53].

8.5 Management of Hyperparathyroidism

Routine blood chemistry screening has been behind the recent increase in the recognition of hyperparathyroidism. Surgery is the major and only current curative modality in treating primary hyperparathyroidism. It is recommended for all patients who are operative candidates and for many asymptomatic patients. Parathyroidectomy is successful in more than 90% of cases in experienced hands, based on intraoperative localization by the surgeon. Identifying the glands can be difficult, however, particularly with removal of multiple glands and with reoperation [54]. Three important factors contribute to successful surgical explorations: correct preoperative diagnosis, accurate preoperative localization of abnormal glands, and meticulous surgical technique [2]. Although the success rate is high in experienced hands, up to 25% of the initial explorations fail because the abnormal glands cannot be located. Prolonged exploration was also found to result in a high incidence of recurrent laryngeal nerve damage [54]. Surgical reexploration with violated anatomy is even more

difficult and hazardous, and can often be unrewarding. Preoperative localization of parathyroid lesions is thus desirable to reduce the incidence of missed lesions and to help avoid prolonged neck exploration. Since surgeons' experience with neck exploration is dwindling due to the reduced incidence of thyroid surgery with the expanding use of iodine-131 for therapy of hyperthyroidism, preoperative localization of parathyroid lesions is even more important than before.

In recent years, minimal access parathyroid surgery(small incisions with gamma probe or endoscopic assistance) is increasingly becoming the operation of choice for single parathyroid adenomas [55]. Compared with bilateral neck exploration it has a shorter hospital stay, less morbidity, and better cosmetic result [56]. The development of this minimally invasive surgical technique has placed an even greater emphasis on preoperative localization [57]. The forms that preoperative localization can take include computed tomography (CT), ultrasound, magnetic resonance imaging (MRI), arteriography, selective venous sampling, ^{99m}Tc-sestamibi (MIBI) scintigraphy, ^{18}F-fluorodeoxyglucose positron emission tomography (FDG PET) and ^{11}C-methionine PET.

8.6 Preoperative Localization

Several imaging and nonimaging modalities have been used to localize the abnormal glands and guide the surgeon. Invasive techniques include arteriography and selective venous sampling via neck vein catheterization. Although these techniques are reliable, they are expensive, time consuming, technically difficult, and involve some risks. Noninvasive techniques are many, indicating that none is ideal. In general, older noninvasive techniques such as barium swallow, thermography, ultrasound, computerized tomography, and scintigraphy using selenomethionine-75 have not been considered very useful for preoperative localization. The morphologic imaging modalities, such as CT, ultrasound and MRI, have the disadvantage that they cannot distinguish functional parathyroid tissue from other types of tissue. However, they provide excellent image resolution and contrast. Overall their accuracy is inadequate and varies. Ultrasound, for example, has a wide range of accuracy, with a range of sensitivity between 36% and 76%. Computed tomography has a similar range, between 46% and 76%. More recently, MRI has also been used with a reported sensitivity of 50% – 78% [58 – 62]. The most sensitive technique is the use of MIBI scintigraphy, with reported sensitivities of approximately 90% [63]. Several other nuclear medicine techniques have been used including thallium-201, ^{99m}Tc-pertechnetate, ^{99m}Tc-tetrofosmin (Myoview), ^{99m}Tc-sestamibi and PET. Some advocate the use of both ^{99m}Tc-sestamibi and ultrasound to confirm abnormal parathyroid tissue [64 – 66]. When the use of both techniques is comprehensive, this may not be a cost-effective approach for primary hyperparathyroidism [67]. Many, including our institution, use only ^{99m}Tc-sestamibi if this test localizes the site of parathyroid hyperactivity.

8.6.1 Scintigraphic Imaging Localization

Since a single parathyroid adenoma is the underlying pathology in more than 80% of cases of primary hyperparathyroidism, there would be no need to explore both sides of the neck with potentially increased morbidity if a sensitive imaging modality could localize the abnormal gland preoperatively. Although experienced neck surgeons can achieve a high success rate of parathyroidectomy after bilateral neck exploration without prior localizing study [2, 3], a preoperative localization study would decrease operative time and morbidity and is frequently needed for the minimally invasive surgical approach that is currently practiced with increasing frequency.

Scintigraphy using ^{99m}Tc-sestamibi is currently the preferred nuclear medicine method for parathyroid imaging. It is the most sensitive and cost-effective modality for preoperative localization of hyperfunctioning parathyroid tissue [4 – 6]. If a single parathyroid adenoma is detected, a unilateral scan-directed neck exploration can be performed. Due to a wide variation in scintigraphic techniques [7, 14], the reported sensitivities of MIBI scan range from 80% to 100%. This radiopharmaceutical is a cationic and lipophilic isonitril derivative that was shown to be taken up by abnormal parathyroid cells. Although the exact mechanism is not fully understood, mitochondria have been implicated in its uptake by parathyroid cells [68]. P-glycoprotein, a membrane transport protein encoded for by the multidrug resistance (MDR) gene, may also be additionally responsible for uptake, since it transports other products with structural similarity to ^{99m}Tc-sestamibi [69]. The uptake and retention of ^{99m}Tc-sestamibi by the abnormal neoplastic and hyperplastic lesions are probably due to the alterations in the biology of the abnormal parathyroid cells, as noted earlier, and mitochondria are probably the site of retention. The size of the lesions is also an important factor in their visualization but cannot alone explain the uptake and retention. This rationale is strengthened by the observation that some large adenomas are occasionally not visualized while small ectopic implants are seen by the technique [68]. In a recent study, Takebayashi et al. found the size and the cellularity of the abnormal gland to correlate with its sestamibi uptake [70]. The authors found a significantly higher count ratio in high cellular glands than in low cellular

ones on either early or delayed images. Bénard et al. [71] reported a large adenoma which was missed on MIBI scan seemingly due to a rapid washout along with the presence of a few oxyphil cells. One study which correlated thallium-201 scintigraphy with ultrastructural alterations in hyperfunctioning parathyroid lesions, has suggested that the ability of this scan to localize the abnormal glands might depend upon the amount of mitochondria-rich oxyphil cells [72]. Generally speaking, the uptake mechanisms of thallium-201 and ^{99m}Tc-MIBI differ significantly. That of thallium depends predominantly on Na^+ and K^+ ATPase pump while ^{99m}Tc-MIBI uptake has been related to the mitochondria. Accordingly, the findings regarding the correlation of thallium uptake by parathyroid adenomas and ultrastructural changes may not be applicable to ^{99m}Tc-MIBI.

Carpentier et al. [73] reported positive correlation between MIBI uptake on delayed images with oxyphil cells in parathyroid adenomas. Other studies did not find a correlation between the degree of hypercellularity of oxyphil cell and MIBI uptake [74] or a relation between the percentage of chief and oxyphil cells and scintigraphic findings [75].

Parathyroid lesions detected by ^{201}Tl scintigraphy have been shown to have significantly higher numbers of mitochondria-rich oxyphil cells compared with nonvisualized lesions, indicating further that the uptake depends in part on the metabolic activity of the lesion [76]. Recently our group found that the amount of mitochondria (Fig. 8.2) in adenoma cells correlates with the degree of uptake [77]. Significant P-glycoprotein or multidrug resistance-related protein expression was reported to limit the sensitivity of

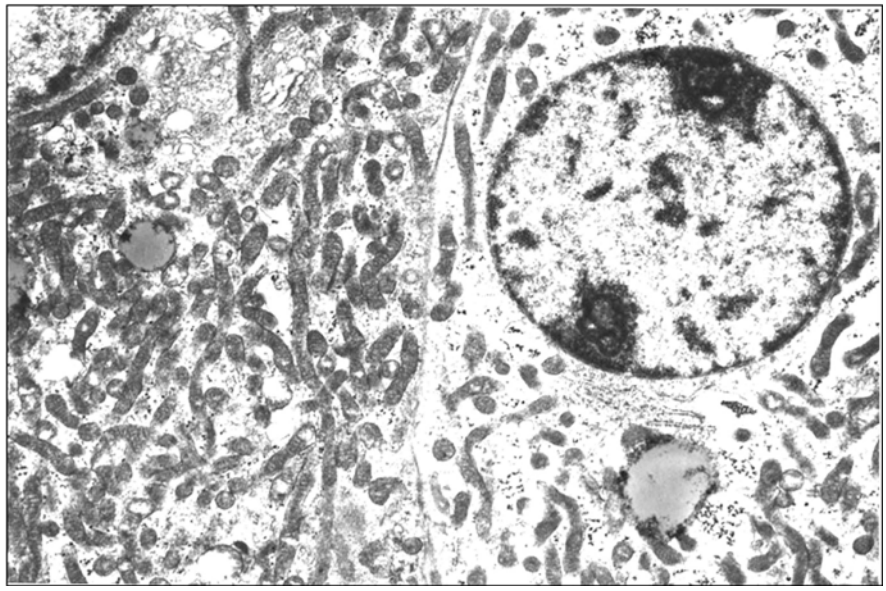

Fig. 8.2. Electron microscopic photograph of a parathyroid adenoma showing cell packed with mitochondria

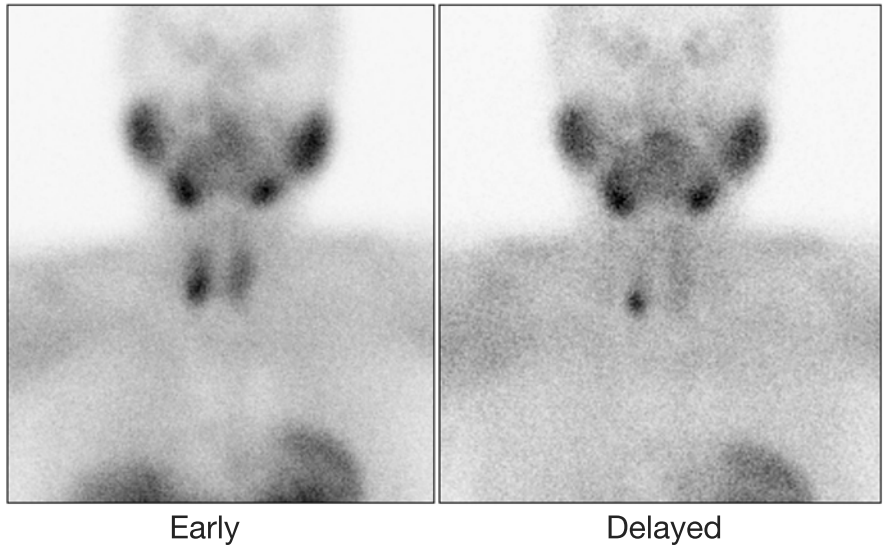

Fig. 8.3. ^{99m}Tc-sestamibi study acquired 15 min and 90 min post-injection. The delayed image shows differential clearance of activity from the thyroid gland with retained and intense uptake by a large parathyroid adenoma of the same patient in Fig. 8.2

^{99m}Tc-MIBI imaging in localizing parathyroid adenomas [78].

Although the activity per gram of tissue in thyroid and parathyroid gland is higher with ^{201}Tl- than with ^{99m}Tc-sestamibi, the slower washout of sestamibi from parathyroid lesions results in a higher target-to-nontarget ratio than with ^{201}Tl [68]. Since the activity in the lesion compared with that in the surrounding tissue affects image contrast, one would expect to distinguish parathyroid lesion from thyroid tissue (Fig. 8.3) better with sestamibi [79] and allow for smaller gland localization. In our experience, switching from ^{201}Tl to ^{99m}Tc-sestamibi resulted in a significant improvement of the accuracy in localizing parathyroid lesions preoperatively.

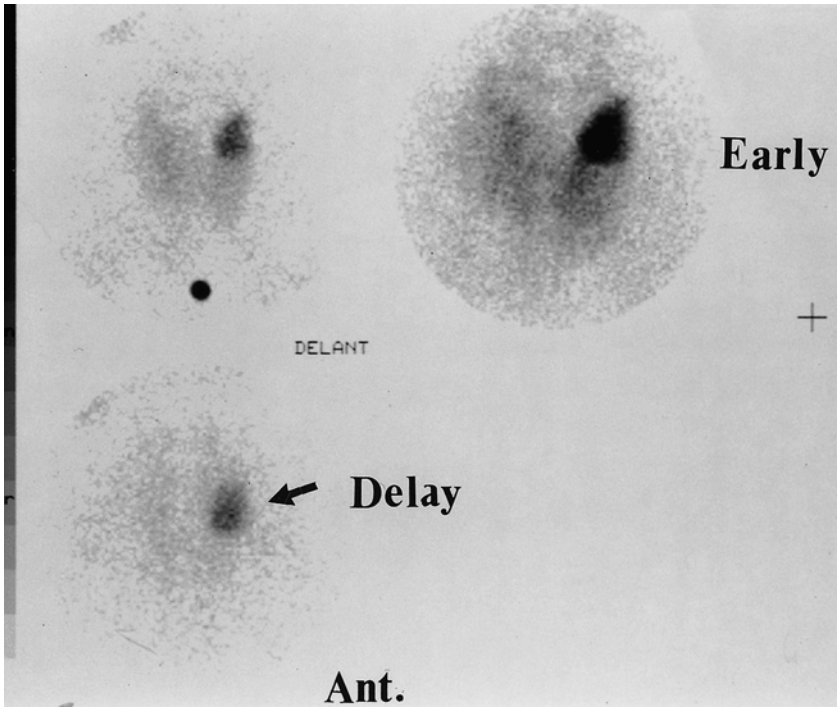

Fig. 8.4. ^{99m}Tc-sestamibi parathyroid localization study showing retained activity in a large parathyroid adenoma (*arrow*) located in left superior position

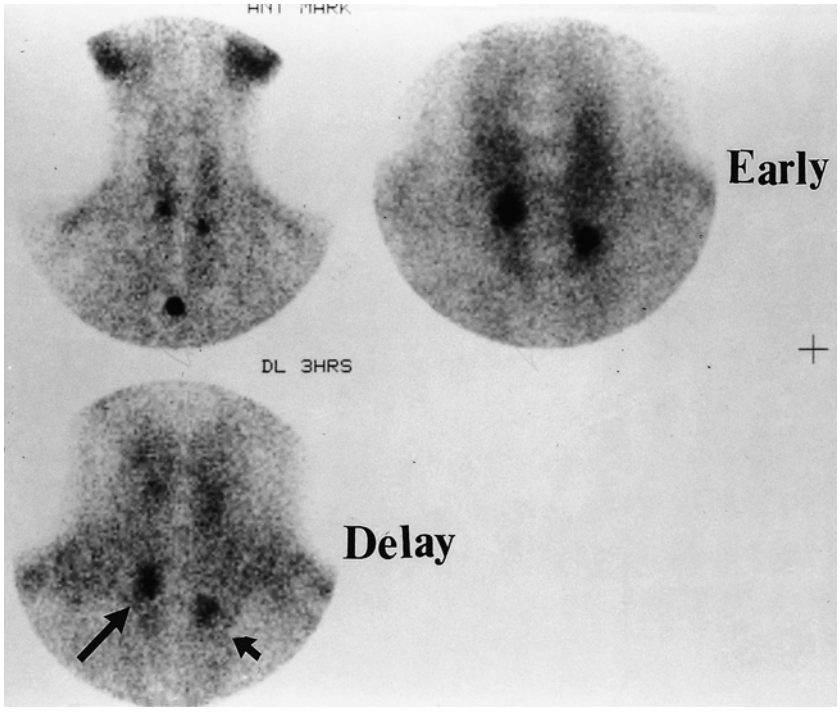

Fig. 8.5. Hyperplastic parathyroid glands (*arrows*) with persistent uptake on delayed ^{99m}Tc-sestamibi image

Parathyroid scintigraphy is not a screening study to be used in each patient with hypercalcemia of unknown etiology. It should be reserved for localization in patients with biochemically proven hyperparathyroidism. Since parathyroid glands can be found ectopically, the search for abnormal parathyroid lesions should include the mediastinal area. Techniques that are based on subtraction such as ^{201}Tl-/^{99m}Tc-pertechnetate are not currently preferred, due to the technical problems associated with subtraction [80, 81]. With the use of ^{99m}Tc-sestamibi, the radiopharmaceutical is injected intravenously and planar images of the neck and chest are obtained at 15 min post-injection with markers of the suprasternal notch, thyroid cartilage, and xiphosternum. Based on the findings, pinhole images of the neck and possibly other areas suspected of having an abnormality are acquired (Figs. 8.4 – 8.6). Images are repeated at 2 – 3 h post-injection, and SPECT is an option when needed for better localization of an abnormality at the discretion of the physician (Fig. 8.7). For planar imaging pinhole collimation is superior to parallel hole collimation [82]. This early and delayed imaging technique is preferred, since the initial uptake by normal thyroid tissue clears while the radiopharmaceutical is usually retained by the abnormal parathyroid cells. This also obviates the need for additional thyroid images using ^{99m}Tc-pertechnetate or ^{123}I with or without subtraction, which are reserved for occasional cases. ^{99m}Tc-tetrofosmin is also being used for scintigraphic localization [83].

Recently PET has been investigated for localizing parathyroid glands. Initial studies using FDG showed conflicting results in imaging the parathyroid glands in primary hyperparathyroidism [84, 85]. ^{11}C-methionine PET was suggested to be more promising than FDG in parathyroid localization. Sundin et al. [86] studied 32 patients with primary hyperparathyroidism, and reported a sensitivity of 85% for proper localization with C-11 methionine. Cook et al. [87] in 8 patients with persistent or recurrent hyperparathyroidism after surgery found that ^{11}C-methionine PET showed all the abnormal parathyroid glands correctly.

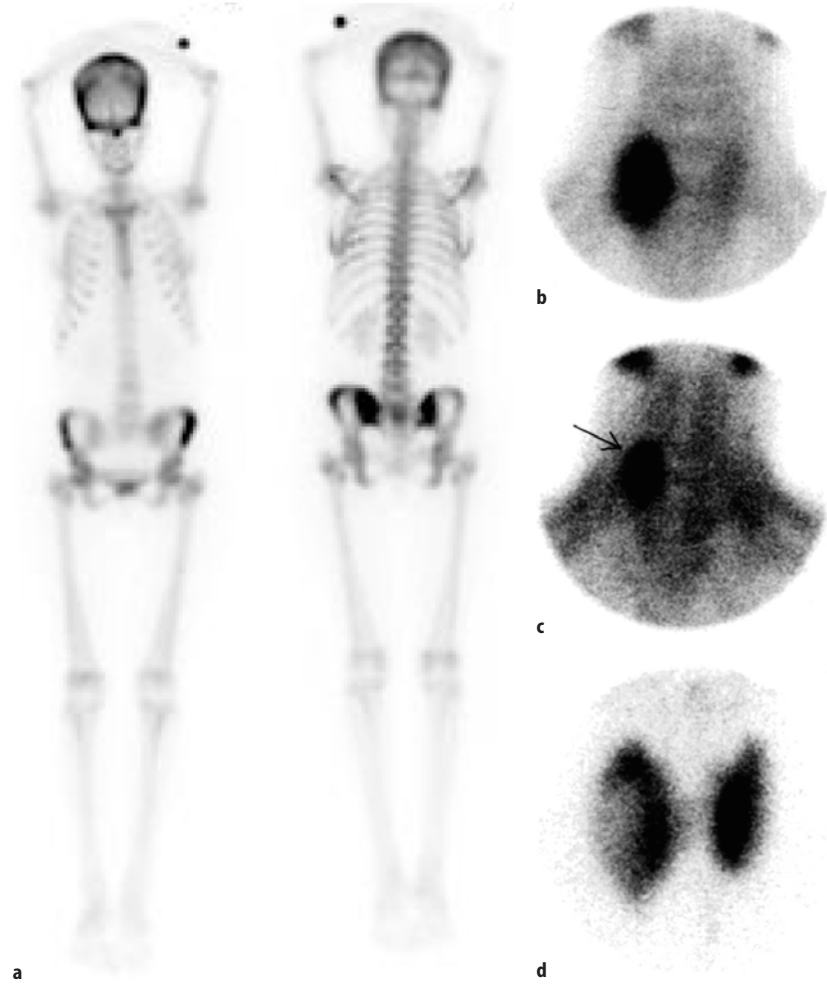

Fig. 8.6a–d. Functioning parathyroid carcinoma. A 45-year-old female was referred for bone scan to evaluate the cause of generalized bony pains. The study (**a**) showed generalized increased bone uptake particularly in the calvarium, indicating metabolic bone disease. Parathyroid hormone was found to be high and ^{99m}Tc-sestamibi (**b-d**) was obtained and showed a focus of increased uptake on early image (**b**) with retention of activity on delayed image (**c**). ^{99m}Tc-pertechnetate thyroid scan (**d**) shows a solitary cold nodule corresponding to the finding on sestamibi study and was proved to be parathyroid carcinoma

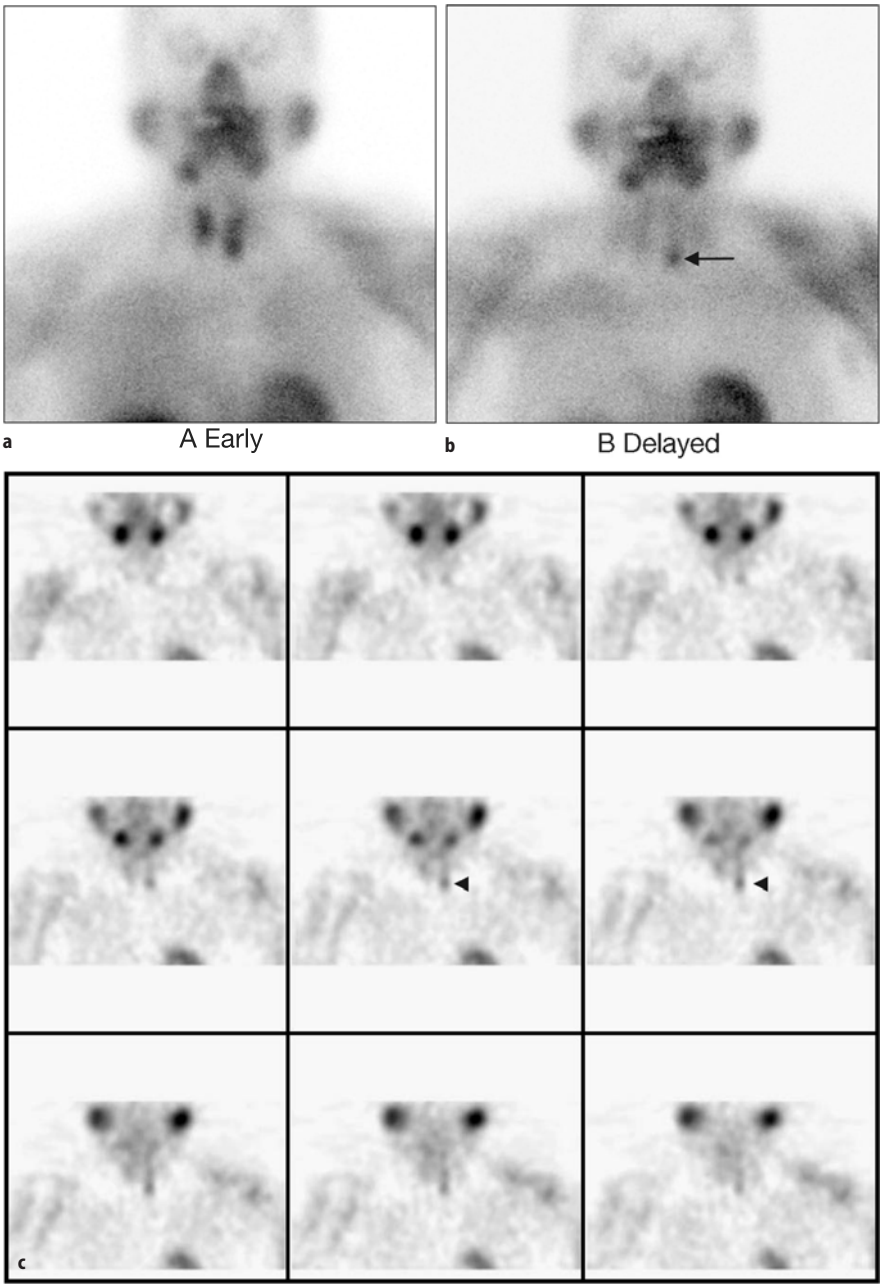

Fig. 8.7a–c. ^{99m}Tc-Sestamibi parathyroid localization study showing retained activity in a parathyroid adenoma (*arrow*) in the left lower pole. SPECT study was obtained. Representative coronal images illustrate the abnormal uptake at the adenoma seen on planar images (*arrowheads*)

More recently Beggs reported a sensitivity of 83%, a specificity of 100% and an accuracy of 88% in successfully locating parathyroid adenomas among 51 patients presenting with hyperparathyroidism, and in whom other imaging techniques including ^{99m}Tc-MIBI had failed to definitely identify the site of adenoma. Most false negatives were due to adenomas in the lower mediastinum that was outside the area of scanning [88].

The protocol for the most popular imaging study ^{99m}Tc-sestamibi parathyroid scintigraphy varies, but in general the technique currently accepted by most researchers is to acquire early static imaging 15 min following injection of 20 mCi ^{99m}Tc-MIBI using a pinhole collimator for the anterior neck and a parallel hole collimator for imaging the mediastinum. This is repeated 2 – 3 h later. Some may still use early dynamic imaging (one frame/min for 60 min) upon i.v. injection of 20 mCi ^{99m}Tc-MIBI using a large-field-of-view gamma camera and a parallel hole collimator. The field should include the neck and mediastinum up to the upper margins of the heart. This dynamic imaging is then followed by planar static images of neck and mediastinum every 20 min until the complete or significant clearance of the radiotracer from the thyroid gland. Advocates of

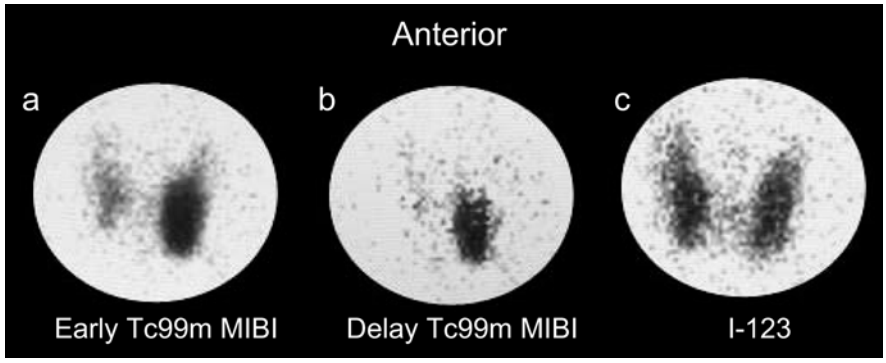

Fig. 8.8a–c. ^{99m}Tc-Sestamibi study shows increased uptake in the left inferior lower pole on early image (**a**) with retention of activity on delayed image (**b**). Iodine-123 4-h study (**c**) acquired on the same day following the sestamibi study shows no thyroid abnormalities. This example illustrates the occasional difficulty in differentiating parathyroid pathology from thyroid abnormalities on sestamibi studies

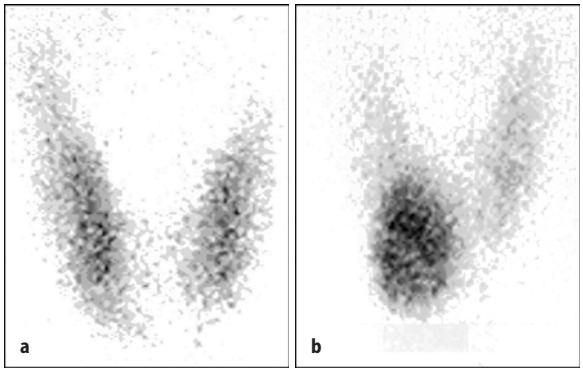

Fig. 8.9a,b. Dual tracer study using ^{99m}Tc-pertechnetate for thyroid scan (a) followed next day by ^{99m}Tc-Myoview acquired as a single early acquisition (**b**). Comparing the two images clearly shows right sided localized accumulation of Myoview with no matching finding on pertechnetate scan. A large parathyroid adenoma was found. This method was reported in a preliminary experience to be easy for interpretation and has high accuracy. (Courtesy of Dr Sahar A-Sobaie)

this protocol think that uptake in some abnormal parathyroid glands shows fast clearance in less than 2 h post-injection. The variable behavior of abnormal parathyroid glands is due to the varying ultrastructure of the cells, the various combinations of cell types, and their biological activity. ^{123}I (Fig. 8.8) or pertechnetate (Fig. 8.6) thyroid imaging for comparison or subtraction is only occasionally needed on an individual basis (e.g., presence of thyroid nodule). If the presence of thyroid pathology is known or suspected clinically, one starts with a thyroid scan to define the morphology and localize the thyroid by injecting 1 mCi ^{99m}Tc-pertechnetate i.v., and the neck is imaged 15 min later.

SPECT imaging has been used routinely or as optional. The study is usually performed acquiring 64 frames (32 × 2 in case of using dual head camera), 30 s each using a matrix of 128× 128 with a circular orbit of 360 degrees. The field of view encompasses the neck and thorax [39]. The additive value of SPECT is controversial [89]. Studies using SPECT showed sensitivities of 53%, 87%, 81%, 57% and 73% respectively [84, 90–93]. It is difficult to know why reported sensitivities differ so much. The low sensitivity reported by De Feo et al. [92] may be secondary to the use of low-dose sestamibi (240 MBq (6.5 mCi) compared with 370–740 MBq (10–20 mCi) for other studies), although Neumann et al. [84] used 740 MBq (20 mCi). The timing of imaging after sestamibi injection may affect sensitivity, but there is no consensus in the literature about optimal timing. Neumann et al. [84] imaged at 10 min, Bonjer et al. [91] at 30 min, De Feo et al. [92] at 10 and 90 min, Kliegler and O'Mara [94] at 30 min and 2 h, Mazzeo et al. [95] at 30 min and 3 h and Slater at 2 h [93]. Tertrofosmin has been also used in a 2-day protocol using ^{99m}Tc-pertechnetete imaging of thyroid and single acquisition of ^{99m}Tc-Myoview next day. Comparing the activity of both scans (Fig. 8.9) obtained 15 min post-injection facilitates detecting focal activity of parathyroid adenomas and hyperplastic glands with high accuracy.

A recent study found that parathyroid sestamibi SPECT scan interpretation by a nuclear medicine physician with an endocrine surgeon resulted in improved accuracy of gland localization and lateralization compared to a nuclear medicine physician reading alone. This improvement may be due to increased awareness of clinical data and head-and-neck anatomy [93].

8.6.2 Intraoperative Probe Localization

Localization using intraoperative gamma probe (Fig. 8.10) has recently gained popularity [96]. The patient is injected 2 h before surgery and the probe is used to detect the higher level of activity after exploration by the surgeon. On the day of surgery, the patients receive the same dose of MIBI as for imaging and are taken to the operating room. Prior to skin incision, counts over four quadrants in the neck as well as over the mediastinum are obtained using a gamma probe [97].

8.6.3 Atypical Washout of Radiotracer

As outlined the diagnosis of parathyroid tumor with ^{99m}Tc-sestamibi scintigraphy is based on the differential washout rate between the thyroid and diseased

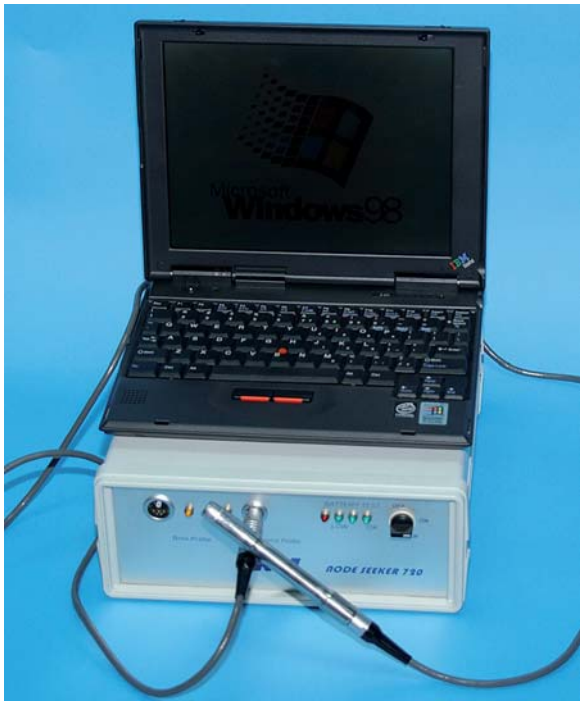

Fig. 8.10. The gamma probe used for intraoperative localization of parathyroid glands in patients with biochemically proven hyperparathyroidism

parathyroids. Atypical radiotracer clearance whether fast parathyroid or delayed thyroid gland washout will limit the efficacy of detection of parathyroid disease with dual-phase ^{99m}Tc-sestamibi scintigraphy as well as using the intraoperative probe.

Early parathyroid washout is frequently seen in parathyroid hyperplasia; the detection rate for this entity is approximately half of that for parathyroid adenoma [52]. Scintigraphy performs worse in cases of multisite hyperplasia, in which only the most prominent radiotracer-avid gland is visualized. In addition, rapid washout from a parathyroid adenoma has been attributed, without unanimous confirmation, to the histologic composition of the adenoma [25, 52]. Modifying the imaging protocol with additional interval scanning between the standard 15-min and 2 – 4-h acquisitions may be helpful in demonstrating rapid washout.

Delayed radiotracer washout from the thyroid parenchyma makes dual-phase scintigraphic assessment difficult. It was observed that the delay varies and significant washout may not occur even several hours after injection of the radiotracer. This retention of ^{99m}Tc-sestamibi occurs in thyroid diseases such as multinodular goiter, Hashimoto thyroiditis, thyroid adenoma, and thyroid carcinoma owing to the hypermetabolic characteristics of these diseases [41, 98, 99]. Extended delayed-phase imaging of ^{99m}Tc-sestamibi along with in-depth clinical examination may be useful in diagnosis of concomitant thyroid and parathyroid disease [100].

Table 8.4. Causes of false-positive ^{99m}Tc-sestamibi [41, 52, 101, 102]

Lymph nodes
Supraclavicular
Axillary
Hyperplastic thymus[a]
Sarcoidosis[b]
Carcinoid tumor
Malignant tumors

[a] Confused with an intrathymic or mediastinal parathyroid adenoma
[b] Thorax

As rapid washout and small size of parathyroid glands would cause false negative localization studies, several pathologies can also cause false positive studies (Table 8.4).

8.7 Summary

To understand the various scintigraphic patterns of parathyroid disease, it is important to understand parathyroid embryology and anatomy. Although experienced neck surgeons can achieve a high success rate of parathyroidectomy after bilateral neck exploration without prior localizing study [2, 3], a preoperative localization study would decrease operative time and morbidity and is frequently needed for the minimally invasive surgical approach that is currently practiced with increasing frequency. The most commonly used and most cost effective modality for preoperative localization is ^{99m}Tc-sestamibi and alternatively ^{99m}Tc-Myoview. The technique is being used before the initial surgery but is most clearly indicated for the preoperative evaluation of recurrent or persistent hyperparathyroidism. SPECT and particularly pinhole acquisition are valuable to improve the accuracy of localization. Intraoperative gamma probe localization is increasingly used also along with the minimally invasive surgical approach. The spectrum of parathyroid disease demonstrated with ^{99m}Tc-sestamibi scintigraphy includes eutopic disease, ectopic disease, solitary adenoma, double or multiple adenomas, cystic adenoma, lipoadenoma, multiple endocrine neoplasia, hyperfunctioning parathyroid transplant and others. The diagnosis of parathyroid tumors with ^{99m}Tc-sestamibi scintigraphy is based on the difference in clearance rates between the thyroid and diseased parathyroid glands, and any condition that interferes with radiotracer clearance will limit the effectiveness of the study. Atypical washout is one of the known entities that can limit the accuracy of these stuidies and it is probably related to the mitochondrial contents of the cells of the abnormal glands.

Adding thyroid scan and ultrasonography improves results but is not cost effective enough to be a routine practice.

Subtraction ^{99m}Tc-sestamibi, iodine-123 scintigraphy or more recently PET may be helpful in difficult cases.

References

1. Carney JA (1996) The glandulae parathyroideae of Ivar Sandstrom. Contributions from two continents. Am J Surg Pathol 20:1123 – 1144
2. Maxon HR, Elgazzar AH (1988) Parathyroid imaging. In: Gelfand G, Thomas S (eds) Effective use of computers in nuclear medicine. McGraw Hill, New York, pp 485 – 496
3. Akerstrom G, Grimelius L, Johansson H, Lundquist H, Pertoft H, Bergstrom R (1981) The parenchymal cell mass in normal human parathyroid glands. Acta Pathol Microbiol Immunol Scand 89(A):367
4. Grimelius L, Ackerstrom Goran, Bonderson L, Juhlin C, Johnsson H, Ljunghall S, Rastad J (1991) The role of the pathologist in diagnosis and surgical decision making in hyperparathyroidism. World J Surg 15:698 – 705
5. Akerstrom G, Rastad J, Ljunghall S, Johnsson H (1990) Clinical and experimental advances in sporadic primary hyperparathyroidism. Acta Chir Scand 156:23 – 28
6. Birkenhager JC, Bouillon R (1996) Asymptomatic hyperparathyroidism. Postgrad Med J 72:323 – 326
7. Mitchell BK, Merrell RC, Kinder BK (1995) Localization studies in patients with hyperparathyroidism. Endocr Surg 75:483 – 498
8. Smith JR. Oates ME (2004) Radionuclide imaging of the parathyroid glands: patterns, pearls, and pitfalls. Radiographics 24:1101 – 1115
9. Berland T, Smith SL, Huguet KL (2005) Occult fifth gland intrathyroid parathyroid adenoma identified by gamma probe. Am Surg 71:264 – 266
10. Wang CA (1976) The anatomic basis of parathyroid surgery. Ann Surg 183:271 – 275
11. Akerstrom G, Malmaeus J, Bergstrom R (1984) Surgical anatomy of human parathyroid glands. Surgery 95:15 – 21
12. Delaney SE, Wermers RA, Thompson GB, Hodgson SF, Dinneen SF (1999) Mediastinal parathyroid carcinoma. Endocr Pract 5:133 – 136
13. Quiros RM, Warren W, Prinz RA (2004) Excision of a mediastinal parathyroid gland with use of video-assisted thoracoscopy, intraoperative 99mTc-sestamibi scanning, and intraoperative monitoring of intact parathyroid hormone. Endocr Pract 10:45 – 48
14. Akerstrom G, Rudberg C, Grimelius L, et al (1986) Histologic parathyroid abnormalities in an autopsy series. Hum Pathol 17:520 – 527
15. Heath H III (1991) Clinical spectrum of primary hyperparathyroidism: evolution with changes in medical practice and technology. J Bone Miner Res 6:S63–S70
16. Fitzpatrick LA (1989) Hypercalcemia in the multiple endocrine neoplasia syndromes. Endocrinol Metab Clin North Am 18:741 – 752
17. Skogseid B, Rastad J, Oberg K (1994) Multiple endocrine neoplasia type 1. Endocrinol Metab Clin North Am 23:1 – 17
18. Herfarth KK, Wells SA (1997) Parathyroid glands and the multiple endocrine neoplasia syndromes and familial hypocalciuric hypercalcemia. Semin Surg Oncol 13:114 – 124
19. Mallette LE (1994) Management of hyperparathyroidism in multiple endocrine neoplasia syndromes and other familial endocrinopathies. Endocrinol Metab Clin North Am 23:19 – 36
20. Duh QY, Hybarger CP, Geist R, Gamsu G, Goodman PC, Gooding GA, Clark OH (1987) Carcinoids associated with multiple endocrine neoplasia syndromes. Am J Surg 154:142 – 148
21. Beus KS, Stack BC (2004) Synchronous thyroid pathology in patients presenting with primary hyperparathyroidism. Am J Otolaryngol 25:308 – 312
22. Nishiyama RH, Farhi D, Thompson NW (1979) Radiation exposure and the simultaneous occurrence of primary hyperparathyroidism and thyroid nodules. Surg Clin North Am 59:65 – 75
23. Prinz RA, Barbato AL, Braithwaite SS (1982) Simultaneous primary hyperparathyroidism and nodular thyroid disease. Surgery 92:454 – 458
24. Attie JN, Vardhan R (1993) Association of hyperparathyroidism with nonmedullary thyroid carcinoma: Review of 31 cases. Head Neck 15:20 – 23
25. Burmeister LA, Sandberg M, Carty SE (1997) Thyroid carcinoma found at parathyroidecomy: Association with primary, secondary and tertiary hyperparathyroidism. Cancer 79:1611 – 1616
26. Sidhu S, Campbell P (2000) Thyroid pathology associated with primary hyperparathyroidism. Aust N Z J Surg 70: 285 – 287
27. Bentrem DJ, Angelos P, Talamonti MS (2002) Is preoperative investigation of the thyroid justified in patients undergoing parathyroidectomy for hyperparathyroidism? Thyroid 12:1109 – 1112
28. Arem R, Lim-Abrahan MA, Mallette LE (1986) Concomitant Graves' disease and primary hyperparathyroidism. Influence of hyperthyroidism on serum calcium and parathyroid hormone. Am J Med 80:693 – 698
29. Ogburn P, Black B (1956) Primary hyperparathyroidism and papillary adenocarcinoma of the thyroid: Report of four cases. Mayo Clin Proc 31:295 – 298
30. Hedman IL, Tisell LE (1984) Associated hyperparathyroidism and non-medullary thyroid carcinoma: The etiological role of radiation. Surgery 95:392 – 397
31. Beus KS, Stack BC Jr (2004) Synchronous thyroid pathology in patients presenting with primary hyperparathyroidism. Am J Otolaryngol 25:308 – 312
32. Sy WM, Mittal AK (1975) Bone scan in chronic dialysis patients with evidence of secondary hyperparathyroidism and renal osteodystrophy. Br J Radiol 48:878 – 884
33. Thompson NW, Eckhauser FE, Harness JK (1982) The anatomy of primary hyperparathyroidism. Surgery 92: 814 – 821
34. Simeone DM, Sandelin K, Thompson NW (1995) Undescended superior parathyroid gland: a potential cause of failed cervical exploration for hyperparathyroidism. Surgery 118:949 – 956
35. Shen W, Duren M, Morita E, Higgins C, Duh QY, Siperstein AE, Clark OH (1996) Reoperation for persistent or recurrent primary hyperparathyroidism. Arch Surg 131:861 – 869
36. Doppman JL, Skarulis MC, Chen CC, et al (1996) Parathyroid adenomas in the aortopulmonary window. Radiology 201:456 – 462
37. Tezelman S, Shen W, Shaver JK, et al (1993) Double parathyroid adenomas: clinical and biochemical characteristics before and after parathyroidectomy. Ann Surg 218: 300 – 309
38. Bartsch D, Nies C, Hasse C, et al (1995) Clinical and surgical aspects of double adenoma in patients with primary hyperparathyroidism. Br J Surg 82:926 – 929

39. Nguyen BD (1999) Parathyroid imaging with Tc-99m sestamibi planar and SPECT scintigraphy. Radiographics 19:601 – 614
40. Clark OH, Duh QY (1989) Primary hyperparathyroidism: a surgical perspective. Endocrinol Metab Clin North Am 18:701 – 714
41. McHenry CR, Lee K, Saadey J, et al (1996) Parathyroid localization with technetium-99m-sestamibi: a prospective evaluation. J Am Coll Surg 183:25 – 30
42. Bergenfelz A, Tennvall J, Valdermarsson S, et al (1997) Sestamibi versus thallium subtraction scintigraphy in parathyroid localization: a prospective comparative study in patients with predominantly mild primary hyperparathyroidism. Surgery 121:601 – 605
43. Rogers LA, Fetter BF, Peete WPJ (1969) Parathyroid cyst and cystic degeneration of parathyroid adenoma. Arch Pathol 88:476 – 479
44. Fallon MD, Haines JW, Teitelbaum SL (1982) Cystic parathyroid gland hyperplasia-hyperparathyroidism presenting as a neck mass. Am J Clin Pathol 77:104 – 107
45. Turner WJD, Baergen RN, Pellitteri PK, Orloff LA (1996) Parathyroid lipoadenoma: case report and review of the literature. Otolaryngol Head Neck Surg 114:313 – 316
46. Cummings C et al (2005) Otolaryngology: head and neck surgery, 4th edn. Mosby, Philadelphia
47. Rinsho N (1995) Primary hyperparathyroidism, pathologic findings and ultrastructure. Jpn J Clin Med 53:861 – 863
48. Baglin A, Junien C, Prinseau J (1991) Mechanism of parathyroid cell proliferation in primary hyperparathyroidism. Presse Med 20:803 – 808
49. Lack CA, Rarber JL, Rubin E (1999) The endocrine system. In: Rubin E, Farber JL (eds) Pathology, 3rd edn. Lippincott-Raven, Philadelphia, pp 1179 – 1183
50. Kilgore EJ, Teigen EL, Cowan RJ (1996) Imaging of transplanted parathyroid tissue in a patient with recurrent hyperparathyroidism. Clin Nucl Med 21:383 – 386
51. Chen CC, Premkumar A, Hill SC, Skarulis MC, Spiegel AM (1995) Tc-99m sestamibi imaging of a hyperfunctioning parathyroid autograft with Doppler ultrasound and MRI correlation. Clin Nucl Med 20:222 – 225
52. Lee VS, Spritzer CE, Coleman RE, Wilkinson RH Jr, Coogan AC, Leight GS Jr (1995) Hyperparathyroidism in high-risk surgical patients: evaluation with double-phase technetium-99m sestamibi imaging. Radiology 197:627 – 633
53. Walker RP, Paloyan E, Gopalsami C (2004) Symptoms in patients with primary hyperparathyroidism: muscle weakness or sleepiness. Endocrine Pract 10:404 – 408
54. Wang CA (1977) Parathyroid re-exploration: a clinical and pathological study of 112 cases. Ann Surg 186:140
55. Assalia A, Inabnet WB (2004) Endoscopic parathyroidectomy. Otolaryngol Clin North Am 37:871 – 886
56. Thomas SK, Wishart GC (2003) Trends in surgical techniques. Nucl Med Commun 24:115 – 119
57. O'Doherty MJ, Kettle AG (2003) Parathyroid imaging: preoperative localisation. Nucl Med Commun 24:125 – 131
58. Erdman WA, Breslau NA, Weinreb JC, Weatherall P, Setiawan H, Harrell R, Snyder W (1989) Noninvasive localization of parathyroid adenomas: a comparison of X-ray computerized tomography, ultrasound, scintigraphy and MRI. Magn Reson Imaging 7:187 – 194
59. Auffermann W, Gooding GA, Okerlund MD, Clark OH, Thurnher S, Levin KE, Higgins CB (1988) Diagnosis of recurrent hyperparathyroidism: comparison of MR imaging and other imaging techniques. Am J Roentgenol 150: 1027 – 1033
60. Peck WW, Higgins CR, Fisher MR, Ling M, Okerland MD, Clark OH (1987) Hyperparathyroidism: comparison of MR imaging with radionuclide scanning. Radiology 163:415 – 420
61. Levin KE, Gooding GA, Okerlund M, Higgins CB, Norman D, Newton TH, Duh QY, Arnaud CD, Siperstein AE, Zeng QH, et al. (1987) Localizing studies in patients with persistent or recurrent hyperparathyroidism. Surgery 102:917 – 925
62. Miller DL, Doppman JR, Shawker TH, Krudy AG, Norton JA, Vucich JJ, et al (1987) Localization of parathyroid adenomas in patients who have undergone surgery, part I. Noninvasive imaging methods. Radiology 162:133 – 137
63. Coakley AJ (2003) Nuclear medicine and parathyroid surgery: a change in practice. Nucl Med Commun 24:111 – 113
64. Van Vroonhoven TJ (2000) Minimally invasive adenomectomy: An alternative for patients with primary hyperparathyroidism. Ann Surg 231:559 – 565
65. Haciyanli M, Lal G, Morita E (2003) Accuracy of preoperative localization studies and intraoperative parathyroid hormone assay in patients with primary hyperparathyroidism and double adenoma. J Am Coll Surg 197:739 – 746
66. Bentrem DJ, Angelos P, Talamonti MS (2002) Is preoperative investigation of the thyroid justified in patients undergoing parathyroidectomy for hyperparathyroidism? Thyroid 12:1109 – 1112
67. Ruda JM, Stack BC Jr, Hollenbeak CS (2004) The cost-effectiveness of sestamibi scanning compared to bilateral neck exploration for the treatment of primary hyperparathyroidism. Otolaryngol Clin North Am 37:855 – 870
68. O'Doherty MJ, Kettle AG, Wells P, Collins RE, Coakley AJ (1992) Parathyroid imaging with technetium 99m-sestamibi: preoperative localization and tissue uptake studies. J Nucl Med 33:313 – 318
69. Piwnica-Worms D, Chiu ML, Budding M, Kronauge JF, Kramer RA, Croop JM (1993) Functional imaging of multidrug resistant P-glycoprotein with an organotechnetium complex. Cancer Res 53:977 – 984
70. Takebayashi S, Hidai H, Chiba T, Takaga Y, Nagatani Y, Matsubara S (1999) Hyperfunctional parathyroid glands with Tc-99m MIBI scan: semiquantitative analysis correlated with histologic findings. J Nucl Med 40:1792 – 1797
71. Bernard F, Lefebvre B, Beuvon F, Langlois MF, Bisson G (1995) Rapid washout of technetium 99m MIBI from a large parathyroid adenoma. J Nucl Med 36:241 – 243
72. Sandrock D, Merino MJ, Norton JA, Neumann RD (1993) Ultrastructural histology correlates with results of thallium-201/Tc-99m parathyroid subtraction scintigraphy. J Nucl Med 34:24 – 29
73. Carpentier A, Jeannotte S, Verrault J, Lefebvre B, Bisson G, Mongeau CJ, et al (1998) Preoperative localization of parathyroid lesions in hyperparathyroidism: relationship between technetium-99m-MIBI and oxyphil cell count. J Nucl Med 39:1441 – 1444
74. Ishibashi M, Nishida H, Okuda S, Suekane S, Hayabuchi N (1998) Localization of parathyroid glands in hemodialysis patients using Tc-99m sestamibi imaging. Nephron 78:48 – 53
75. Pinero A, Rodriguez JM, Ortiz S, Soria T, Bermejo J, Claver MA, et al (2000) Relation of biochemical, cytologic, and morphologic parameters to the result of gammagraphy with technetium 99m sestamibi in primary hyperparathyroidism. Otolaryngol Head Neck Surg 122:851 – 855
76. Sandrock D, Merino MJ, Norton JA, Neumann RD (1993) Ultrastructural histology correlates with results of thallium-201/technetium-99m parathyroid subtraction scintigraphy. J Nucl Med 34:24 – 29
77. Naddaf S, Anim JJ, Farghaly MM, Behbehani AE, Alshomar KA, Elgazzar AH (2005) Ultrastructure of hyperfunctioning parathyroid glands: does it explain various patterns of sestamibi uptake JNM 45:P
78. Kao A, Shiau YC, Tsai SC, Wang JJ, Ho ST (2002) Technetium-99m methoxyisobutylisonitrile imaging for parathy-

roid adenoma: relationship to P-glycoprotein or multidrug resistance-related protein expression. Eur J Nucl Med Mol Imaging 29:1012 – 1015
79. Goris ML, Basso LV, Keeling C (1991) Parathyroid imaging. J Nucl Med 32:887 – 889
80. Elgazzar AH, Maxon HR, Hertzberg V, et al (1985) Parathyroid scintigraphy with and without thyroid hormone suppression. Proceedings of the Eastern Great Lakes Chapter, Society of Nuclear Medicine, Niagara Falls, New York
81. Thule P, Thakore K, Vansant J, McGarity W, Weber C, Phillips LS (1993) Preoperative localization of parathyroid tissue with technetium-99m sestamibi I-123 subtraction scanning. J Clin Endocrinol Metab 78:77 – 82
82. Dontu VS, Kettle AG, O'Doherty MJ, Coakley AJ (2004) Optimization of parathyroid imaging by simultaneous dual energy planar and single photon emission tomography. Nucl Med Commun 25:1089 – 1093
83. Al-Sobaei S (2005) Proceedings of the first gulf nuclear medicine congress. Riyadh, Saudi Arabia, March 1 – 3
84. Neumann DR, Esselstyn CB, MacIntyre WJ, Go RT, Obuchowski NA, Chen EQ, et al (1996) Comparison of FDG-PET and sestamibi SPECT in primary hyperparathyroidism. J Nucl Med 37:1809 – 1815
85. Melon P, Luxen A, Hamoir E, Meurisse M (1995) Fluorine-18-fluorodeoxyglucose positron emission tomography for preoperative parathyroid imaging in primary hyperparathyroidism. Eur J Nucl Med 22:556 – 558
86. Sundin A, Johansson C, Hellman P, Bergstrom M, Ahlstrom H, Jacobson GB, et al (1996) PET and parathyroid L-[carbon-11]methionine accumulation in hyperparathyroidism. J Nucl Med 37:1766 – 1770
87. Cook GJR, Wong JCH, Smellie WJB, Young AE, Maisey MN, Fogelman I (1998) [^{11}C]Methionine positron emission tomography for patients with persistent or recurrent hyperparathyroidism. Eur J Endocrinol 139:195 – 197
88. Beggs AD, Hain SF (2005) Localization of parathyroid adenomas using ^{11}C-methionine positron emission tomography. Nucl Med Commun 26:133 – 136
89. Melton GB, Somervell H, Friedman KP, Zeiger MA, Cahid CA (2005) Interpretation of ^{99m}Tc sestamibi parathyroid SPECT scan is improved when read by the surgeon and nuclear medicine physician together. Nucl Med Commun 26:633 – 638
90. Civelek AC, Ozalp E, Donovan P, Udelsman R (2002) Prospective evaluation of delayed technetium-99m sestamibi SPECT scintigraphy for preoperative localization of primary hyperthyroidism. Surgery 131:149 – 157
91. Bonjer HJ, Bruining HA, Valkema R, Lameris JS, de Herder WW, van der Harst E, Pols HA (1997) Single radionuclide scintigraphy with 99m-technetium-sestamibi and ultrasonography in hyperparathyroidism. Eur J Surg 163:27 – 32
92. De Feo ML, Colagrande S, Biagini C, Tonarelli A, Bisi G, Vaggelli L, Borrelli D, Cicchi P, Tonelli F, Amorosi A, Serio M, Brandi ML (2000) Parathyroid glands: combination of ^{99m}Tc MIBI scintigraphy and US for demonstration of parathyroid glands and nodules. Radiology 214:393 – 402
93. Slater A, Gleeson FV (2005) Increased sensitivity and confidence of SPECT over planar imaging in dual-phase sestamibi for parathyroid adenoma detection. Clin Nucl Med 30:1 – 3
94. Klieger P, O'Mara R (1998) The diagnostic utility of dual phase Tc-99m sestamibi parathyroid imaging. Clin Nucl Med 23:208 – 211
95. Mazzeo S, Caramella D, Lencioni R, Molea N, De Liperi A, Marcocci C, Miccoli P, Iacconi P, Bossio GB, Viacava P, Lazzeri E, Bartolozzi C (1996) Comparison among sonography, double-tracer subtraction scintigraphy, and double-phase scintigraphy in the detection of parathyroid lesions. AJR Am J Roentgenol 166:1465 – 1470
96. Berland T, Smith SL, Huguet KL (2005) Occult fifth gland intrathyroid parathyroid adenoma identified by gamma probe. Am Surg 71:264 – 266
97. Ugur O, Bozkurt MF, Hamaloglu E, Sokmensuer C, Etikan I, Ugur Y, Sayek I, Gulec SA (2004) Clinicopathologic and radiopharmacokinetic factors affecting gamma probe-guided parathyroidectomy. Arch Surg 139:1175 – 1179
98. Bergenfelz A, Tennvall J, Valdermarsson S, et al (1997) Sestamibi versus thallium subtraction scintigraphy in parathyroid localization: a prospective comparative study in patients with predominantly mild primary hyperparathyroidism. Surgery 121:601 – 605
99. Taillefer R, Boucher Y, Potvin C, Lambert R (1992) Detection and localization of parathyroid adenomas in patients with hyperparathyroidism using a single radionuclide imaging procedure with technetium-99m-sestamibi (double-phase study). J Nucl Med 33:1801 – 1807
100. Caixas A, Berna L, Hernandez A, Tebar FJ, Madariaga P, Vegazo O, Bittini AL, Moreno B, Faure E, Abos D, Piera J, Rodriguez JM, Farrerons J, Puig-Domingo M (1997) Efficacy of preoperative diagnostic imaging localization of technetium 99m-sestamibi scintigraphy in hyperparathyroidism. Surgery 121:535 – 541
101. Mudun A, Kocak M, Unal S, Cantez S (1995) Tc-99m MIBI accumulation in remnant thymus: a cause of false-positive interpretation in parathyroid imaging. Clin Nucl Med 20:379 – 380
102. Desai S, Yuille DL (1993) Visualization of a recurrent carcinoid tumor and an occult distant metastasis by technetium-99m-sestamibi. J Nucl Med 34:1748 – 1750